

Self-consistent $\pi N t$ matrix

J. W. Van Orden, M. K. Banerjee, D. M. Schneider, and S. J. Wallace

Department of Physics and Astronomy, University of Maryland, College Park, Maryland 20742

(Received 2 September 1980)

The πN interaction in the nuclear medium is shown to be substantially altered by local field effects, including dressing of internal pion lines by the optical potential. The local field effect arises due to scattering of pions in the intermediate states of the $\pi N t$ matrix from other nucleons in the medium. We develop an organization of pion scattering theory based on Goldstone diagrams which includes all possible contributions but emphasizes the dressing of propagators in $\pi N t$ -matrix intermediate states involving one pion and one nucleon only. Pion absorption and rescattering are treated on an equal footing. Self-consistency is introduced through the demand that the optical potential which dresses internal propagators be the same as the optical potential which is implied by the t matrix so corrected. For calculational purposes, the general theory is simplified to the case of the $\pi N t$ matrix in a Fermi gas. The input data consist of the free $\pi N t$ matrix, an off-shell form factor, the πN coupling constant, a binding energy, and a Fermi momentum k_F . Nucleon recoil effects are retained, as they have previously been found to be important. Numerical results are presented for the quantity $W(k, \omega)$ which is related to the Klein-Gordon optical potential for nuclear matter. The results show substantial modification of the πN resonance by the nuclear medium. In particular, the resonance is broadened and the treatment of pion absorption provides sensible results for the imaginary part of the self-energy near threshold. Our calculations show the self-consistency is not crucial to the results, as dressing of propagators by the first-order optical potential is adequate. Nucleon recoil is significant. The results show that local field effects are important in π -nucleus interactions.

[NUCLEAR REACTIONS General π -nucleus scattering theory, self-consistent
 $\pi N t$ matrix, absorption, nucleon recoil, Pauli effects, propagator dressing,
 optical potential.]

I. INTRODUCTION

Theories of pion-nucleus scattering have generally developed within two organizational frameworks; one is multiple scattering theory,¹ and the other is the isobar-hole approach.² Although the approaches are interrelated at a formal level, they present quite different organizations of the important physics.

Multiple scattering theory emphasizes the role of quasifree πN interactions in a nucleus. Although numerous corrections enter, the essential input to multiple scattering approaches is the free $\pi N t$ matrix with appropriate off-shell behavior. The $t\rho$ optical potential can be calculated with relatively little ambiguity and provides a start towards understanding many gross features of pion elastic scattering data. Recent analyses³ have also emphasized the need for a secondary term, thought to be representative of π absorption, in order to obtain good fits to elastic scattering data. The large reaction cross section for π absorption⁴ underlines this need in a very direct way. Generally, absorption contributions to the optical potential have been treated on a phenomenological level, particularly in cases where the πN dynamics are modeled by a separable potential theory.

The second approach—*isobar hole theory*—focuses on the formation of Δ isobars in the nucleus, in direct analogy to the particle-hole excitations

which are conventional in nuclear physics. The Δ isobar is treated on similar footing to a stable particle; however, the isobar interaction with the nuclear medium is emphasized, and generally the mass and width parameters of the isobar are substantially altered by the nuclear interaction. The principal difference between multiple scattering and isobar-hole approaches therefore lies in the relative emphasis on alteration of the πN interaction (isobar) due to nuclear interactions.

In the multiple scattering approach, medium-dependent shifts of πN resonance parameters arise due to higher order terms which have been called local field corrections.⁵ These terms describe the modification of the intermediate states of the $\pi N t$ matrix due to multiple scattering of the π from other nucleons. Alternatively, one may view the process as a self-energy dressing of the pion propagation in the intermediate state of the $\pi N t$ matrix due to the local field produced by other nucleons. Putting aside nuclear recoil corrections, the pion self-energy becomes the same as the π -nucleus optical potential, and the local field corrections provide a microscopic theory for the modification of the πN resonance due to the nuclear medium. Keister,⁶ Johnson and Bethe,⁷ and Johnson and Keister⁸ have exhibited the role of local field corrections in a particularly simple model (fixed scatterers in nuclear matter). However, the local field corrections are, in fact, much too large when examined in the fixed scatterer limit. The

leading order local field contributions to the $\pi^{-16}\text{O}$ optical potential is 3.5 times as big as the "leading" $t\rho$ term at the resonance energy. Several effects regulate this divergent behavior of the multiple scattering series, the principal one being nucleon recoil. Including nucleon recoil effects, Banerjee and Wallace⁹ have shown that the local field correction is reduced by a factor of 7 in $\pi^{-16}\text{O}$, but still ends up being about two-thirds the magnitude of the leading $t\rho$ term of the optical potential. Multiple scattering expansions may converge, but too slowly to be very practical, at least near the resonance energy. Thus, there are two main lessons which have emerged from the previous work on local field corrections in π -nucleus scattering: (i) a nonstatic treatment of the nucleons is required; (ii) the local field effects should be summed to all orders of multiple scattering in terms of a self-energy which dresses all pion propagators. These points form the foundation of this work on the self-consistent π -nucleus optical potential.

The idea of self-consistency is simply that the optical potential and the self-energy insertion which dresses the pion propagator should be identical. Johnson and Bethe⁷ used this idea to regulate the excessive local field effects which arise in the fixed scatterer approach to pion scattering. As will become apparent, self-consistency may not be a central issue. In the present work the dressing of pion propagators by the first-order optical potential gives results which differ little from the fully self-consistent results.

Celenza, Liu, Nutt, and Shakin¹⁰ previously considered the modification of the separable potential $\pi N t$ matrix in nuclear matter due to the dressing of pion propagators by the first order optical potential. They found substantial broadening of the resonance similar to that of the present study. However, our emphasis differs in several respects, most importantly by inclusion of the pion absorption mechanism on an equal footing with the πN scattering mechanism. Any complete treatment of the π -nucleus optical potential requires a treatment of the absorption processes. Correlations between nucleons are usually thought to play an important role in the description of π absorption. However, there is also a substantial two-nucleon contribution to π absorption which does not involve correlations, and this process can be incorporated into the self-consistent π -nucleus optical potential on the same footing as the resonant πN scattering contribution. In work which will be reported elsewhere,¹¹ we show that recoil effects tend to lessen the role of correlations in pion absorption. In the present work, only the pion absorption due to uncorrelated pairs will be

dealt with directly; however, our general approach can readily include other contributions.

The strategy of this paper is to consider, for the first time, the basic pion scattering and absorption contributions to the π -nucleus optical potential in a nonperturbative fashion. More exotic effects due to correlations, intermediate ρ mesons, and crossed pion insertions are not included in this initial work. Thus, the only parameters which enter are those required to parametrize the $\pi N t$ matrix by a pole and right-hand cut contribution. Apart from the off-shell form factor, all the input is determined by the πN phase shifts and the πN coupling constant.

The paper is organized as follows. A general theoretical framework for the self-consistent $\pi N t$ matrix is developed in Sec. II A. The theory is developed in some detail using Goldstone diagrams in order to provide a clear basis for calculations, although a number of aspects of the general theory are well known. The absorption pole diagrams are included and the general theory is so organized that the final equations have all the simplicities of a theory based on potentials. The reader who is more interested in the approximate equations which form the basis for our calculation may skip to Sec. II B. Section III A details the calculation of the self-consistent t matrix in nuclear matter using several simplifying approximations, and Sec. III B presents the results. Conclusions are discussed in Sec. IV.

II. THEORY

A. Introduction to a self-consistent theory of the $\pi N t$ matrix

A new organization of the theory of pion-nucleus interactions is necessary to embed self-consistently the $\pi N t$ matrix into the nuclear medium. In this section, a concise account of the theory is presented in terms of Goldstone diagrams. For the convenience of the reader a partial summary of these rules,¹² needed for understanding this paper, is given in Appendix A.

The set of all diagrams describing the free space $\pi N t$ matrix modified by closing the external nucleon lines to form a loop generates a very important subset of diagrams describing the $\pi N t$ matrix in a nucleus. This subset will be represented with a hatched circle as shown in Fig. 1. Figure 2(a) is an example of one particularly simple Goldstone diagram (pole term) occurring in the free $\pi N t$ matrix. Here the vacuum is the true vacuum. A fermion line directed upward represents a nucleon and a fermion line directed downward represents an antinucleon. Figure 2(b) shows the corresponding contribution in the nucleus, and

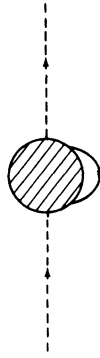


FIG. 1. Goldstone diagram representing the first-order optical potential (self-energy). Dashed lines are pions, downward direct solid line represents a nucleon hole. Hatched circle represents the free $\pi N t$ matrix.

in this case the vacuum stands for the nucleus in the ground state. The upward directed fermion lines represent nucleons above the Fermi sea (particle states). Downward directed lines represent the creation of holes not only in the Fermi sea but also in the filled negative energy sea (antinucleons). The contribution of the latter in Fig. 2(b) normally would be a part of pion mass renormalization, but it is not the same as in free space because it is modified by Pauli blocking and, therefore, will not be completely canceled by the pion mass counter term. The difference is precisely the contribution to π -nucleus scattering coming from the Z -graph mechanism of πN scattering. The contribution of the holes in the Fermi sea to Fig. 2(b) represents the more familiar nucleon pole term. The preceding remarks show how antinucleons can come into play, and how one does the necessary bookkeeping; however, in the rest of the paper we never again refer to antinucleons. Only the part of the downward directed lines which contain the holes in the Fermi sea will be retained, since the purpose of this paper is to discuss the in-

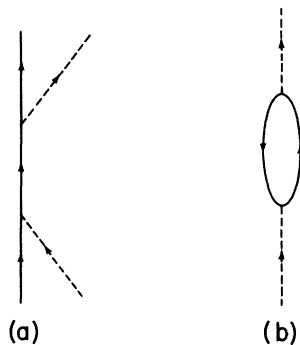


FIG. 2. Goldstone diagram representing the nucleon pole contribution to the free $\pi N t$ matrix (a) and the corresponding Goldstone diagram in the nuclear medium.

fluence of the nuclear medium on the πN interaction.

The set of Goldstone diagrams collectively represented by the hatched circle of Fig. 1 differs from the complete set of Feynman diagrams for the free $\pi N t$ matrix in two respects. First, the diagrams of Fig. 1 incorporate several effects of the nuclear medium such as Pauli blocking and binding effects. Second, the diagrams contain a factor of $(1/2\omega_r)^{1/2}$ for each external pion line and, in principle, a factor of $[M/E(p)]^{1/2}$ for each external nucleon line; however, we take the nucleon motion to be nonrelativistic and omit the second factor.

A few more remarks are in order to help us appreciate the role of Fig. 1 in the description of π -nucleus scattering. For every direct diagram in Fig. 1 there is a crossed diagram where the entry and the exit points of the external pion are interchanged. The set of crossed diagrams is indicated in Fig. 3. If we decided to keep our physics at the simple level of the mechanisms indicated by Figs. 1 and 3, one might suspect that the sum of the two sets of diagrams would be the Schrödinger optical potential. This is incorrect because chains of the sort shown in Fig. 4, with all connecting pion lines moving upward, are not enough, and one must also include twists in the chain as shown in Fig. 5. Reference 12 showed that when the twists are included, the pion propagation is described by a Klein-Gordon equation, the "potential" for which is the sum of Figs. 1 and 3, but without the factors of $(1/2\omega_r)^{1/2}$ from the rule regarding external pion lines. Therefore, the sum of Figs. 1 and 3, which represents the pion self-energy in the nuclear medium, is related to the Klein-Gordon optical potential by a simple factor. For this reason the terms "self-energy" and "optical potential" will be used interchangeably in this paper.

The purpose of the present paper is to go beyond

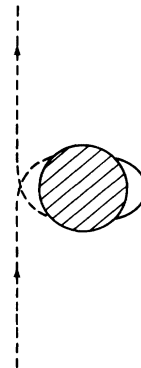


FIG. 3. Diagram representing the crossing of the processes represented by Fig. 1.

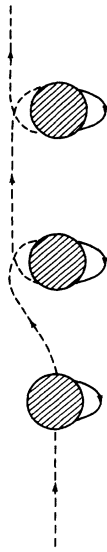


FIG. 4. A diagram generated by using a Schrödinger π -nucleus optical potential consisting of the sum of Figs. 1 and 3.

the approximation of using Figs. 1 and 3 as the source of the π -nucleus optical potential. The complete set of all diagrams which make up the optical potential will be denoted by Fig. 6, where the hatched rectangular box represents the full $\pi N t$ matrix in the nuclear medium and the direct and the crossed set are represented in the previously adopted manner. It is convenient to separate the diagrams of Fig. 6 into two categories.

Category 1 contains the set of Fig. 1 and all

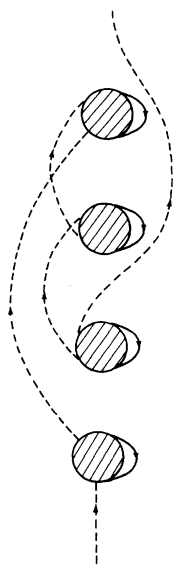


FIG. 5. A diagram which cannot be generated by the optical potential described in the caption to Fig. 4.

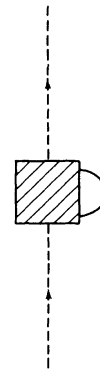


FIG. 6. Goldstone diagram representing the complete π -nucleus optical potential. The hatched square represents the complete $\pi N t$ matrix in the nuclear medium.

other diagrams which one can generate by letting one of the internal lines, π or N , of a diagram of Fig. 1, have one or more elastic interactions with the nuclear medium. In this paper we ignore the elastic interactions of internal nucleon lines for simplicity. The elastic interaction of an internal pion line with the nuclear medium can be any irreducible diagram (i.e., not containing two parts connected solely by a pion line) inserted into a pion line which does not connect with other lines in the main diagram. A complete set of these irreducible diagrams is necessarily equal to the set represented by the hatched rectangular box in Fig. 6, and this is precisely how self-consistency comes into the problem. Figure 7(a) shows a simple element of Fig. 1; Fig. 7(b) shows a complete elastic interaction inserted once; and Fig. 7(c) shows the interaction inserted twice. When all orders of insertions are included, the internal pion line is *fully dressed*. Of course, the full

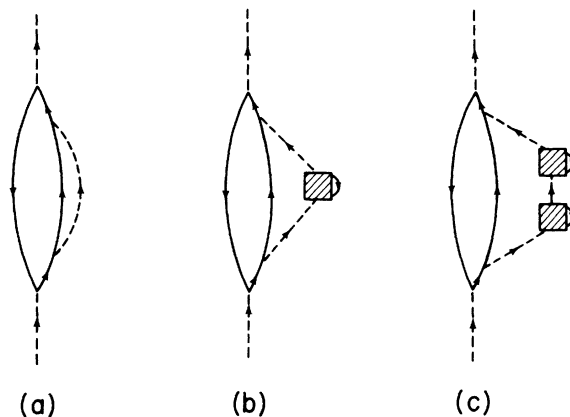


FIG. 7. Some diagrams represented by the diagram of Fig. 6, which illustrate the dressing of internal pion lines.

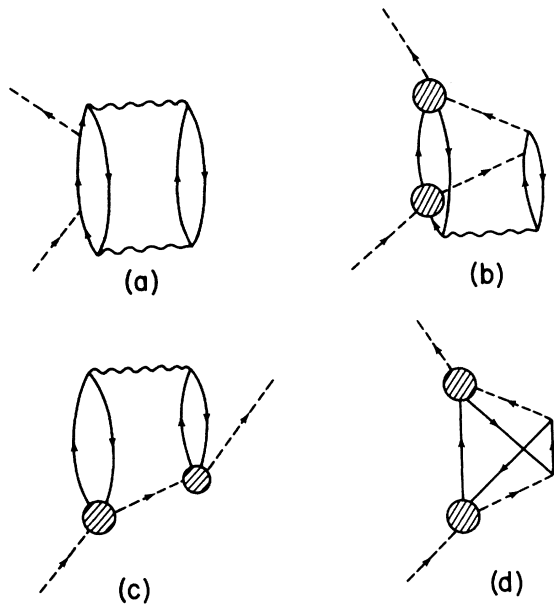


FIG. 8. Some other diagrams which are represented by Fig. 6 and which belong to category 2.

dressing requires inclusion of insertions of the type shown in Figs. 4 and 5.

Category 2 contains all other irreducible diagrams which contribute to the optical potential of Fig. 6. A few examples are given in Fig. 8. Figure 8(a) represents absorption and then emission of a pion by a correlated nucleon pair. The solid wavy line represents the nucleon-nucleon G matrix and this interaction plays an important role in providing the momentum required in the π absorption process. In Fig. 8(b) the πN scattering serves that purpose. The NN interaction correlates the motion of the two nucleons and has other important effects. Figure 8(c) represents a piece of double scattering of π by a correlated nucleon pair and is an important part of the well-known

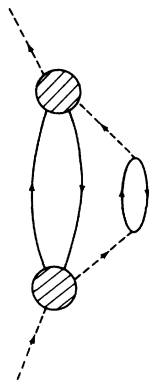


FIG. 9. An absorption diagram belonging to category 1.

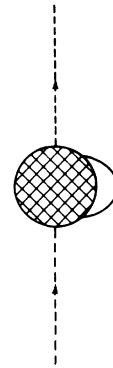


FIG. 10. The cross hatched circle represents all contributions to the $\pi N t$ matrix in the nuclear medium which do *not* contain elastic (one pion-one particle-one hole) intermediate states where the pion propagator is dressed.

Lorentz-Lorenz Ericson-Ericson (LLEE) effect. Figure 8(d) results from nucleon exchange in a diagram which belongs to category 1 (see Fig. 9).

We now introduce a tactical simplification for the purpose of the present paper only. This involves dropping all crossed graphs which are not internal to Fig. 1. The crossed graphs internal to Fig. 1 are included in the calculations of this paper since we obtain all of our πN amplitudes from the measured physical amplitudes. In a subsequent paper we will show how to include the other crossed graphs; however, dropping them simplifies the problem considerably and is well worth doing at this developmental stage. We do *not* intend to convey any impression that the crossed graphs are unimportant, however.

The next step is to identify a subset of the diagrams of Fig. 6 which have the following feature: there is no elastic interaction inserted on an in-

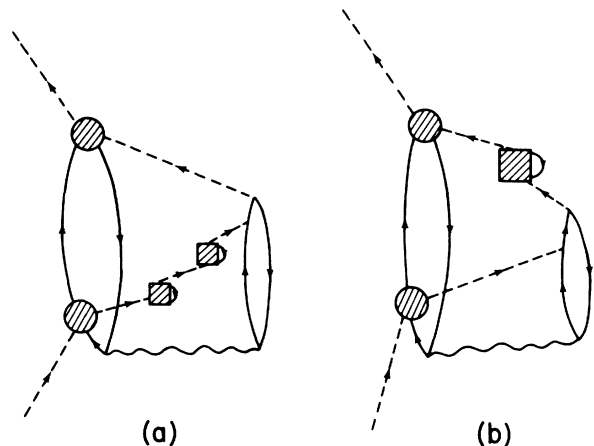


FIG. 11. (a) A diagram which is contained in Fig. 10, and (b) a diagram which is not contained in Fig. 10.

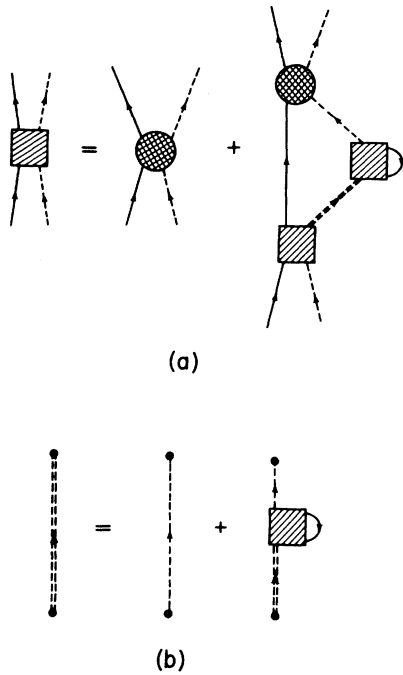


FIG. 12. Diagrammatic representation of the self-consistent t matrix equations.

ternal pion line if at the same time only one particle-hole pair and nothing else is present. This subset is represented by Fig. 10. The set contains all of Fig. 1. It contains all diagrams of category 2 with bare internal pion lines, such as the ones shown in Figs. 8. Some of the internal pion lines can be dressed. Thus, it can contain Fig. 11(a) but not Fig. 11(b), because in the latter the elastic interaction is inserted when we have only one particle-hole pair besides the internal pion.

The $\pi N t$ matrix, represented by the cross hatched circle of Fig. 10, therefore contains the subset of all diagrams contributing to the full $\pi N t$

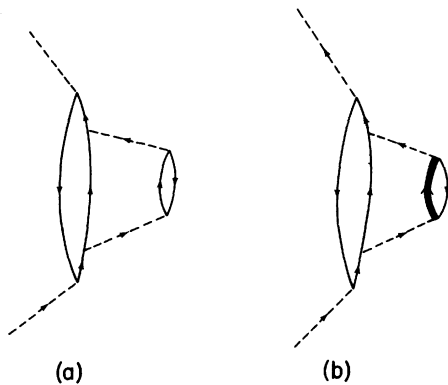


FIG. 13. Diagrams illustrating possible double counting of potential contributions by the self-consistent equation.

matrix in the medium, represented by the hatched box of Fig. 6, which do not contain a dressed pion line in any one-nucleon-one-pion (elastic) intermediate state. The reason for grouping the diagrams in this manner is that the dressing of the pion lines in the elastic intermediate states can then be accomplished through a linear equation which is amenable to solution as a practical matter. The complete set of diagrams for the $\pi N t$ matrix in the nuclear medium is then given by the diagrammatic self-consistent equation represented by Fig. 12(a) where the double dashed line represents a fully dressed pion line as given by the linear equation displayed diagrammatically in Fig. 12(b). The diagrams shown in Fig. 12 represent the linear self-consistent equation

$$T_{\pi N}^{SC} = T_{\pi N}^D + T_{\pi N}^D (G_{\pi N}^{SC} - G_{\pi N}^P) T_{\pi N}^{SC}, \quad (1)$$

where $T_{\pi N}^{SC}$ is the self-consistent t matrix represented by the hatched square, $T_{\pi N}^D$ is the t matrix resulting from the processes represented by the cross hatched circle, $G_{\pi N}^P$ is the Pauli corrected πN propagator, and $G_{\pi N}^{SC}$ is the self-consistent πN propagator which depends upon the self-consistent self-energy. Equation (1) is very general, as it simply expresses the replacement of the Pauli-corrected propagator $G_{\pi N}^P$ in the elastic intermediate states by the fully dressed propagator $G_{\pi N}^{SC}$. The theory can always be so organized.

In the general framework represented diagrammatically in Fig. 12, nuclear potential insertions in the nucleon lines have been neglected on the grounds that the effective interaction for particles above the Fermi sea is weak. In the context of nuclear matter, Brandow¹³ has argued that this is

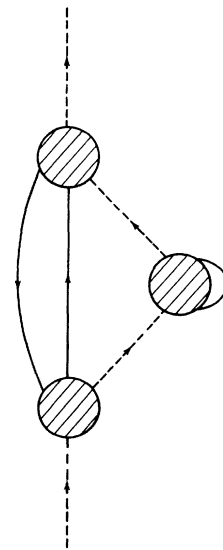


FIG. 14. Goldstone diagram representing the local field correction.

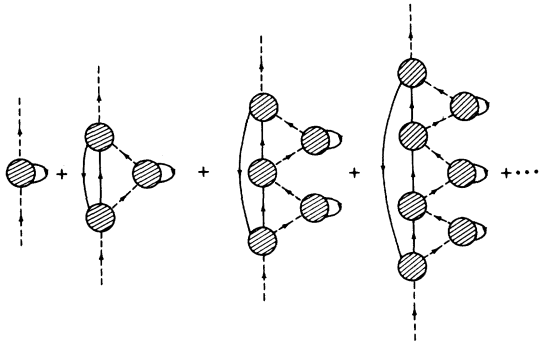


FIG. 15. Diagrams representing the local field series.

a reasonable choice. However, it is important to note that one cannot avoid additional potential-like insertions on the nucleon lines being generated by the self-consistent theory when the nucleon pole term is included in the $\pi N t$ matrix. Some examples of this are given in Fig. 13.

Figure 13(a) indicates the leading order local field correction due to pion absorption obtained when we consider the nucleon pole terms for the circle and boxes in Fig. 12(a) and use the free pion propagator for all pion lines. This diagram is similar to one for a two-pion exchange potential insertion on the nucleon line. Similarly, Fig. 13 (b) shows the leading order local field correction due to pion rescattering via the isobar (right-hand cut) portion of the t matrix. This diagram is similar to one for another part of the two-pion exchange potential insertion on the nucleon line. Thus, the general framework of the self-consistent equations of Fig. 12 automatically generates

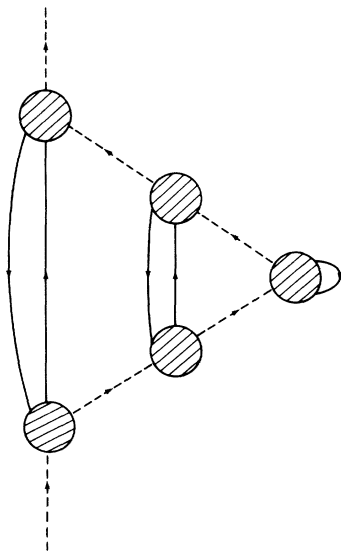


FIG. 16. A complicated diagram illustrating the need for self-consistency.

some parts of the potential insertions on the nucleon line. If the same parts were already included via a potential insertion on the nucleon lines, there would be double counting. Our present treatment of the dressing of the nucleon line due to NN interaction is so simplistic that it is pointless to dwell on this question. At this stage we merely note that the question of double counting is inseparable from the question of the correct NN interaction to be used in the appropriate kinematical regime, and we leave such questions to the future. As a practical matter the difficulty is not very important in the numerical calculations of Sec. III, as may be gauged by the small energy shift of the nucleon pole part of the self-consistent t matrix away from the free pole energy. This energy shift of the pole will be discussed later in this paper. In particular, the imaginary part of the optical potential is expected to be relatively insensitive to these questions.

B. Dominant contributions to the self-consistent $\pi N t$ matrix

Having presented the general theory of the self-consistent t matrix, it is instructive to consider some of the important diagrams which contribute to the self-consistent self-energy represented by Fig. 6 in more detail. In order to simplify the discussion presented in the remainder of this paper, we will assume that the set of diagrams represented by the cross hatched circle of Fig. 10 is well approximated by the Pauli-corrected t matrix represented by the hatched circle of Fig. 1. This assumption amounts to neglecting contributions to the driving term (cross hatched circle) from correlated multiple scatterings such as those shown in Fig. 11 and processes involving other than elastic (one particle-one hole-one pion) intermediate states. The relative importance of correlated double scattering (LLEE) and correlated absorption contributions is reported in two other papers.^{11,14}

The simplest contribution to the π nucleus optical potential which involves nuclear particle-hole excitations is shown by the Goldstone diagram in Fig. 14. Here the incoming pion scatters from a nucleon in the Fermi sea, exciting a particle-hole pair. The pion then scatters elastically from a second nucleon in the Fermi sea before rescattering from the first nucleon to leave the nucleus in the ground state. This process is called the local field correction,⁵ as calculated by Keister,⁶ and Banerjee and Wallace.⁹

In order to obtain a reasonable value for the local field correction and to ensure that unitarity is maintained, it is necessary to consider an infinite sequence of these events such as shown in

Fig. 15. This series contains the first-order optical potential plus the lowest order local field correction plus diagrams containing two or more "reflections" of the intermediate pion by other nucleons but always returning to the first nucleon. We refer to this set of diagrams as the *local field series*. It should be noted here that such a series is included naturally in the isobar-hole formalism by means of the isobar self-energy. Indeed, the equivalent of the local field series is generated if the lowest order pion self-energy is used to calculate the isobar self-energy, as is the case in the calculation of Oset and Weise.¹⁵

In the local field series, as described above, each reflection of the intermediate pions consist of only one elastic interaction of the pion with another nucleon before returning to the first nucleon. It is, of course, possible for the pion to undergo any number of elastic interactions with other nucleons before rescattering from the first nucleon, as is illustrated by Fig. 7. The effect of including all such elastic interactions is the "dressing" of the internal pion lines.

An example of another type of local field diagram is shown in Fig. 16. In this figure the incoming pion scatters from a nucleon in the Fermi sea, exciting a particle-hole pair. The pion proceeds to a second nucleon and scatters creating a second particle-hole pair. The pion then interacts elastically from a third nucleon before returning to the second nucleon to deexcite the second particle-hole pair. It then returns to the first nucleon to rescatter, leaving the nucleus in the ground state. Alternately, this may be viewed as the intermediate pion interacting with the nuclear medium by means of the lowest order local field correction term before returning to the first nucleon. The point is that intermediate pions can be scattered from the nuclear medium by the same processes associated with the optical potential seen by incident pions. Therefore, the determination of the optical potential must be done self-consistently.

Pauli corrections to the $\pi N t$ matrix can be approximated in a well-known manner.¹⁶ It is always possible to organize the diagrams contributing to the free $\pi N t$ matrix in such a manner that the free t matrix can be found by solving a Lippman-Schwinger-type equation

$$T_{\pi N}^0 = D + DG_{\pi N}^0 T_{\pi N}^0, \quad (2)$$

where $T_{\pi N}^0$ is the free $\pi N t$ matrix, $G_{\pi N}^0$ is the free πN propagator, and D is a driving term. In order to obtain this form, the driving term D contains all diagrams which do not have any one-pion-one nucleon (elastic) intermediate states. This organization emphasizes the importance of the elastic (πN) intermediate states through the πN propagator

in the second term of (2) and is very much in the same spirit as the organization of the self-consistent equation presented above. It is, of course, not convenient to solve Eq. (2), but this organization facilitates the introduction of Pauli corrections by allowing one the calculational advantages of a potential theory without resorting to the use of a potential theory. A similar equation can be written for the Pauli-corrected t matrix:

$$T_{\pi N}^P = D + DG_{\pi N}^P T_{\pi N}^P, \quad (3)$$

where $T_{\pi N}^P$ is the Pauli-corrected $\pi N t$ matrix and $G_{\pi N}^P$ is the Pauli-corrected πN propagator. In writing this equation it is assumed that the major contribution to Pauli corrections comes from the elastic (πN) intermediate states. By using the same driving term D in Eqs. (2) and (3), Pauli corrections to inelastic and nucleon pole intermediate states are neglected. It can be argued that since pions in multiple pion intermediate states must have a rather high total momentum in the c.m. frame, any nucleon in such a state must also have a large momentum and will be little influenced by Pauli blocking. Therefore, it is reasonable to ignore Pauli corrections to these terms. Equations (2) and (3) can be formally combined to eliminate the driving term D . This leads to the equation

$$T_{\pi N}^P = T_{\pi N}^0 - T_{\pi N}^0 \frac{1 - Q}{E - K_{\pi} - K_N + i\eta} T_{\pi N}^P, \quad (4)$$

where E is the starting energy of the πN system, $K_{\pi} = (m_{\pi}^2 - \nabla_{\pi}^2)^{1/2}$, $K_N = -\nabla_N^2/2M$, and Q is the Pauli operator which projects onto unoccupied states. This method can be recognized as the matrix inversion method used in the nuclear many-body problem¹⁷

When the Pauli-corrected amplitude $T_{\pi N}^P$ of Eq. (4) is used to approximate the set of πN reducible diagrams $T_{\pi N}^D$, the self-consistent equation (1) becomes

$$T_{\pi N} = T_{\pi N}^P + T_{\pi N}^P \left(\frac{Q}{E - K_{\pi} - K_N - \Sigma(\omega - K_N) + i\eta} - \frac{Q}{E - K_{\pi} - K_N + i\eta} \right) T_{\pi N}, \quad (5)$$

where $T_{\pi N}$ is the self-consistent $\pi N t$ matrix. The cross hatched circle of Fig. 12 is approximated by the Pauli-corrected t matrix $T_{\pi N}^P$, and Σ is the self-consistent pion self-energy obtained from $T_{\pi N}$. A specific example is worked out in the next section. A similar set of equations has been proposed by Celenza *et al.*¹⁰

III. A SIMPLE SOLVABLE EXAMPLE

A. The nuclear matter case

Our discussion up to this point has concerned only general considerations relating to the self-consistent t matrix and has been independent of any particular models for the nucleus or for the free πN t matrix. Before proceeding to solve Eq. (4) for Pauli corrections and Eq. (5) for the self-consistent t matrix using the nuclear shell model and a more sophisticated treatment of the free t matrix, it is instructive to consider the solution of these equations within the context of a simple solvable model. This model, as presented below, contains the basic elements of the self-consistent calculation so that the solution should exhibit the same qualitative features as the more complicated

problem while not necessarily being quantitatively accurate. This allows one to gain some feeling for the relative importance of the various elements and features of the self-consistent solution before one tackles the more complicated problem.

In order to simplify the solution of the Pauli correction equation (4) and the self-consistent equation (5), we use the Fermi gas model of the nucleus which has only the Fermi momentum k_F and the binding energy B as parameters. Use of the Fermi gas model requires that all elastic pion scatterings in the Fermi sea must be forward scatterings. In keeping with the motivation of this calculation, nucleons are allowed to recoil. We are *not* using the fixed scatterer approximation.

In the Fermi gas model the Pauli correction equation (4) becomes

$$\hat{T}_{\pi N}^P(k'\beta, k\alpha; p', p) = \hat{T}_{\pi N}^0(k'\beta, k\alpha; p', p) + \frac{1}{(2\pi)^3} \sum_{\gamma} \int d^3q \hat{T}_{\pi N}^0(k'\beta, q\gamma; p', p+k-q) \times \frac{\theta(|\vec{p} + \vec{k} - \vec{q}| - k_F) - 1}{\omega + E(\vec{p}) - E(\vec{p} + \vec{k} - \vec{q}) - \omega_q + i\eta} \hat{T}_{\pi N}^P(q\gamma, k\alpha; p+k-q, p) \quad (6)$$

and the self-consistent equation (5) becomes

$$\hat{T}_{\pi N}^0(k'\beta, k\alpha; p', p) = \hat{T}_{\pi N}^P(k'\beta, k\alpha; p', p) + \frac{1}{(2\pi)^3} \sum_{\gamma} \int d^3q \hat{T}_{\pi N}^P(k'\beta, q\gamma; p', p+k-q) \theta(|\vec{p} + \vec{k} - \vec{q}| - k_F) \times \left(\frac{1}{\omega + E(\vec{p}) - B - E(\vec{p} + \vec{k} - \vec{q}) - \omega_q - \Sigma[\vec{q}, \omega - E(\vec{p}) - B - E(\vec{p} + \vec{k} - \vec{q})] + i\eta} - \frac{1}{\omega + E(\vec{p}) - B - E(\vec{p} + \vec{k} - \vec{q}) - \omega_q + i\eta} \right) \cdot \hat{T}_{\pi N}^0(q\gamma, k\alpha; p+k-q, p), \quad (7)$$

where k and k' are the initial and final pion four-momenta; p and p' are the corresponding nucleon four-momenta; α , β , and γ are pion isospin indices; and the caret denotes that the t matrices are operators in the nucleon spin-isospin space. $E(\vec{p}) = \vec{p}^2/2M$ and $\omega_q = (\vec{q}^2 + m_{\pi}^2)^{1/2}$.

In order to simplify further the solution of (6), only P -wave πN amplitudes are used and the free πN t matrix is taken to be of a static factorable separable form:

$$\hat{T}_{\pi N}^0(k'\beta, k\alpha; p', p) = -4\pi \sum_{I, J} h_{2I, 2J}^0(\omega) \Omega_{2J}(\vec{K}', \vec{K}) \Lambda_2(\beta, \alpha) \times \frac{v(k')}{(2\omega_{k'})^{1/2}} \frac{v(k)}{(2\omega_k)^{1/2}}, \quad (8)$$

where ω is the pion energy, $h_{2I, 2J}^0(\omega)$ is related to the experimental phase shifts by

$$h_{2I, 2J}^0(\omega) = \frac{M + \omega}{M} \frac{\eta_{2I, 2J} e^{2i\delta_{2I, 2J}} - 1}{2i k_{c.m.}^3 v^2(k_{c.m.})}, \quad (9)$$

where

$$k_{c.m.}^2 = \left(\frac{(\omega + M)^2 + m_{\pi}^2 - M^2}{2(M + \omega)} \right)^2 - m_{\pi}^2 \quad (10a)$$

and

$$v(k) = \frac{1}{1 + \vec{k}^2/\mu^2} \quad (10b)$$

is a form factor. μ is the form factor mass and will be chosen to equal the nucleon mass ($\mu = M$) in the calculations presented below.

In Eq. (8) both the isospin (I) and spin (J) indices are understood to be summed over the values $\frac{1}{2}$ and $\frac{3}{2}$. The isospin projection operators $\Lambda_{2I}(\beta, \alpha)$ are

$$\Lambda_1(\beta, \alpha) = \frac{1}{3} \tau_{\beta} \tau_{\alpha}, \quad (11a)$$

$$\Lambda_3(\beta, \alpha) = \delta_{\beta\alpha} - \frac{1}{3} \tau_{\beta} \tau_{\alpha}, \quad (11b)$$

and the static spin projection operators $\Omega_{2J}(\vec{K}', \vec{K})$ are

$$\Omega_1(\mathbf{K}', \mathbf{K}) = \mathbf{K}' \cdot \mathbf{K} + i\sigma \cdot \mathbf{K}' \times \mathbf{K}, \quad (12a)$$

$$\Omega_3(\mathbf{K}', \mathbf{K}) = 2\mathbf{K}' \cdot \mathbf{K} - i\sigma \cdot \mathbf{K}' \times \mathbf{K}. \quad (12b)$$

As a further simplification in this calculation, the spin-dependent parts of the spin projection operators are dropped, giving

$$\Omega_{2J}(\mathbf{K}', \mathbf{K}) \cong (J + \frac{1}{2})\mathbf{K}' \cdot \mathbf{K}. \quad (13)$$

Retaining the spin-flip terms increases the complexity of the coupling of the amplitudes, but adds nothing to the instructional value of the problem.

The energy dependence of the off-shell amplitudes is given by a Low equation for the right-hand cut plus the right-hand nucleon pole term. The nucleon pole term corresponds to the absorption and reemission of a single pion by a single nucleon. This term produces pion absorption contributions to the self-consistent t matrix. The energy dependence of the off-shell amplitudes is then given by

$$h_{2I,2J}^0(\omega) = -\frac{3g_\pi^2(0)}{16\pi M^2\omega} \delta_{I,1/2} \delta_{J,1/2} + \frac{1}{\pi} \int_{m_\pi}^{\infty} dz \frac{\text{Im} h_{2I,2J}^0(z)}{z - \omega - i\eta}, \quad (14)$$

where $g_\pi(0) = 12.7$.

By choosing a static form of the t matrix, effects associated with transformation of variables from the πN c.m. frame to the nuclear rest frame are ignored. When applied to the free t matrix, these Fermi motion effects have been shown to result in a considerable broadening of the resonance as well as an increase in resonant mass.¹⁸ However, local field effects also considerably broaden the free resonance, and thus the self-consistent t matrix is less susceptible to Fermi broadening. Our neglect of this effect should not qualitatively alter the results discussed below. A correct treatment of this effect would greatly increase the complexity.

As a further simplification we make the angle-averaged approximation to the energy denominators

$$E(\vec{p}) - E(\vec{p} + \mathbf{K} - \vec{q}) = \frac{\vec{p}^2}{2M} - \frac{(\vec{p} + \mathbf{K} - \vec{q})^2}{2M} \cong -\frac{(\mathbf{K} - \vec{q})^2}{2M} = -E(\mathbf{K} - \vec{q}) \quad (15)$$

$$F(k, \omega) = \frac{1}{(2\pi)^3} \int \frac{d^3q}{2\omega_q} v^2(q) \frac{(\mathbf{K} \cdot \vec{q})^2}{K^2} \beta^2(|\vec{q} - \mathbf{K}|, k_f) \times \left(\frac{1}{\omega - B - [(\mathbf{K} - \vec{q})^2/(2M)] - \omega_q - \Sigma\{\vec{q}, \omega - B - [(\mathbf{K} - \vec{q})^2/(2M)]\} + i\eta} - \frac{1}{\omega - B - [(\mathbf{K} - \vec{q})^2/(2M)] - \omega_q + i\eta} \right) \quad (22)$$

and replace the theta functions, $\theta(|\vec{p} + \mathbf{K} - \vec{q}| - k_f)$ in (6) and (7), by an effective Fermi function,¹⁹ $\beta^2(|\mathbf{K} - \vec{q}|, k_f)$, where

$$\beta^2(\mathbf{K}, \mathbf{K}_f) = \frac{3}{4} \frac{k}{k_f} \left(1 - \frac{1}{12} \frac{k^2}{k_f^2} \right) \theta(2k_f - k) + \theta(k - 2k_f). \quad (16)$$

Since the free t matrix was chosen to be of a separable form, it is also reasonable to assume, as an ansatz, that the self-consistent t matrix will be of the separable form

$$T_{\pi N}(k'\beta, k\alpha; p', p) = -4\pi \sum_{I,J} h_{2I,2J}(k, \omega) \Omega_{2J}(k', k) \Lambda_{2I}(\beta, \alpha) \times \frac{v(k)}{(2\omega_k)^{1/2}} \frac{v(k')}{(2\omega_{k'})^{1/2}} \quad (17)$$

The Pauli-corrected t matrix is also of this form.

Substituting (8), (16), and (17) into (6) leads to the solution of the Pauli correction equation

$$H_{2I}^P(k, \omega) = \frac{H_{2I}^0(\omega)}{1 + H_{2I}^0(\omega) \mathcal{F}(k, \omega)}, \quad (18)$$

where

$$H_{2I}^{(P)} = 4\pi \sum_J (J + \frac{1}{2}) h_{2I,2J}^{(P)}, \quad (19)$$

and

$$\mathcal{F}(k, \omega) = \frac{1}{(2\pi)^3} \int \frac{d^3q}{2\omega_q} v^2(q) \frac{(\mathbf{K} \cdot \vec{q})^2}{K^2} \times \frac{\beta^2(|\vec{q} - \mathbf{K}|, k_f) - 1}{\omega - [(\mathbf{K} - \vec{q})^2/(2M)] - \omega_q + i\eta}. \quad (20)$$

Note that by using the idempotency relations for the isospin projection operators,¹² separate solutions can be written for each isospin channel. However, the spin quantum numbers are summed because the various spin channels are coupled.

Similarly, the solution of the self-consistent equation (7) becomes

$$H_{2I}(k, \omega) = \frac{H_{2I}^P(k, \omega)}{1 + H_{2I}^P(k, \omega) F(k, \omega)}, \quad (21)$$

where

The self-energy $\Sigma(k, \omega)$, which is related to the Klein-Gordon optical potential $\Pi(k, \omega)$ (the invariant self-energy) by

$$\Pi(k, \omega) = 2\omega_k \Sigma(k, \omega), \quad (23)$$

is defined as

$$\Sigma_{\alpha\beta}(k, \omega) = \sum_{st} \int \frac{d^3p}{(2\pi)^3} \langle st | \hat{T}(k\beta, k\alpha; p, p) | st \rangle, \quad (24)$$

where s and t are the spin and isospin indices of the nucleon.

Using (8) and (17), the self-energy may be written as

$$\Sigma(k, \omega) = -\frac{\mathbb{K}^2}{2\omega_k} v^2(k) W(k, \omega), \quad (25)$$

where we define

$$W(k, \omega) = \frac{2k_f^3}{9\pi^2} \sum_I (I + \frac{1}{2}) H_{2I}(k, \omega - B). \quad (26)$$

Similar equations hold for the free quantities H^0 , W^0 , Σ^0 , and the Pauli-corrected quantities H^P , W^P , Σ^P . The function W which is related to Σ by (25) is dimensionless and weakly dependent upon the pion momentum k .

To obtain a numerical solution to the self-consistent equation, Eqs. (18), (20), (25), and (26) are used to find a Pauli-corrected self-energy. This then gives a first approximation to the self-consistent self-energy needed to calculate F from (22). This in turn can be combined with (21), (25), and (26) to give a new approximation to the self-consistent self-energy in (22). This process is continued until the input and output self-energies are identical.

B. Results for the nuclear matter case

All of our results are presented in terms of the dimensionless quantity $W(k, \omega)$ which is defined by Eq. (26). This is directly related to the self-energy $\Sigma(k, \omega)$ by Eq. (25), and Σ is then related to the Klein-Gordon optical potential π by Eq. (23).

Figures 17–23 show W as a function of the pion energy ω . As noted earlier, $W(k, \omega)$ is a weakly varying function of the pion momentum k . All of the curves shown in these figures are calculated with the Fermi momentum $k_f = 1.9m_\pi c$, the form factor mass μ equal to the nucleon mass M , the binding energy $B = 0.15m_\pi$, and, with a fixed pion momentum, $k = 2m_\pi c$. Solid or broken lines represent the real part of W , while dashed lines represent the imaginary part of W .

Figure 17 shows W as calculated with free (curve 1) and Pauli-corrected (curve 2) t matrices. Comparison of these two calculations below threshold

($\omega < m_\pi$) shows that the primary effect of Pauli corrections in the region is to shift the position of the nucleon pole to higher energy. This shift reflects the effect of Pauli corrections on nucleon mass renormalization in the nuclear medium and is discussed in detail in Appendix B. Above threshold the Pauli-corrected curves have the resonance shifted to higher energy and the resonant width is only approximately 75% of the free value.

Figure 18 shows the effect on W of adding the lowest order self-energy correction shown in Fig. 14 to the Pauli-corrected W . The imaginary parts of both the Pauli-corrected (curve 2) and Pauli-plus-local-field-correction (curve 3) W 's are shown in this figure. It is obvious that the first-order local field correction has a drastic effect on the self-energy, causing $\text{Im}W$ not to have a simple resonant shape. Indeed, $\text{Im}W$ changes sign, indicating that unitarity has been violated. This is the result of two competing processes. By opening a new channel, flux is robbed from the original channel and W is quenched. In addition, the new channel contributes flux to the scattering process in a way that tends to maintain the original sign of the imaginary part of W . In the lowest order local field correction, too much flux is removed without being replaced by the new channel. This causes the imaginary part of W to change sign.

If unitarity is to be maintained, it is necessary to sum the entire local field series as shown in

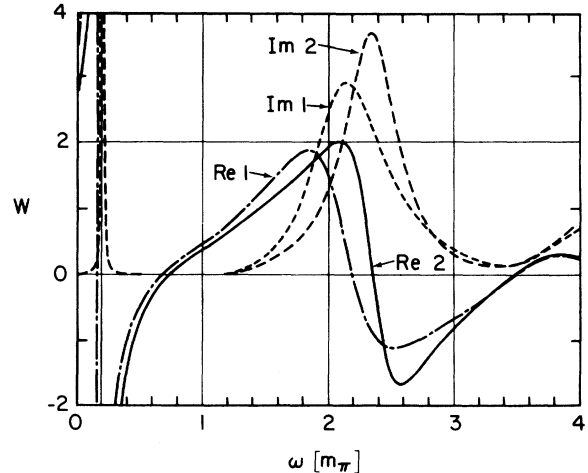


FIG. 17 $W(k, \omega)$ as a function of ω , comparing W calculated with the free $\pi N t$ matrix (curve 1) and the Pauli-corrected W . In this graph, and all those presented hereafter, solid or broken lines represent the real part of W , and dashed lines the imaginary part, $k = 2m_\pi c$, $k_f = 1.9m_\pi c$, and the binding energy $= 0.15m_\pi$. For the relationship of W to the Klein-Gordon optical potential, see Eqs. (23)–(26).

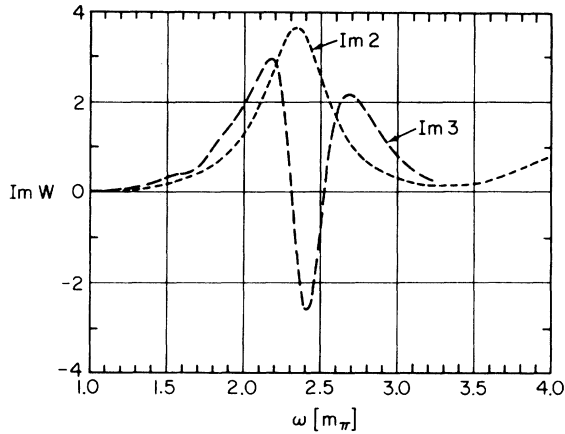


FIG. 18. Pauli-corrected W (curve 2) versus the Pauli-corrected W plus the lowest order local field correction (curve 3). Note that unitarity is violated.

Fig. 15. Figure 19 compares W resulting from the summation of the local field series (curve 4) to the Pauli-corrected W (curve 2). It is clear from this figure that by summing the local field series unitarity is maintained and that W is again roughly of the resonant form.

The next step is to dress the internal pion lines in the local field series using the Pauli-corrected self-energy. This corresponds to the first iteration of the solution of the self-consistent equation. W for the dressed local field series (curve 5) is compared to W for the local field series without dressed pion lines (curve 4) in Fig. 20. The effect of the dressing is a smoothing of the energy variation. Although the general effect may not appear to be large, the dressing may result in a considerable change in the value of W at a given energy. In particular, at the threshold, $\omega = m_\pi$, the imaginary part of W is increased by about a factor of 3 over the bare value. At threshold the imaginary part of W comes entirely from pion absorption in the intermediate states.

Figure 21 illustrates the importance of nucleon recoil in calculating the local field series. This figure compares the dressed local field series (curve 5), as shown in the previous figure, to a similar calculation where the nucleon recoil mass has been doubled (curve 6). The change in $\text{Im}W$ caused by doubling the recoil mass is substantial at threshold and at resonance. It is clear that nucleon recoil must be properly treated in order to evaluate local field effects.

Figure 22 illustrates the convergence of our iterative scheme for solving the self-consistent equation. W is shown for both the first iterate (or dressed local field series, curve 5) and the converged self-consistent solution (curve 7). The two solutions differ only in detail which suggests

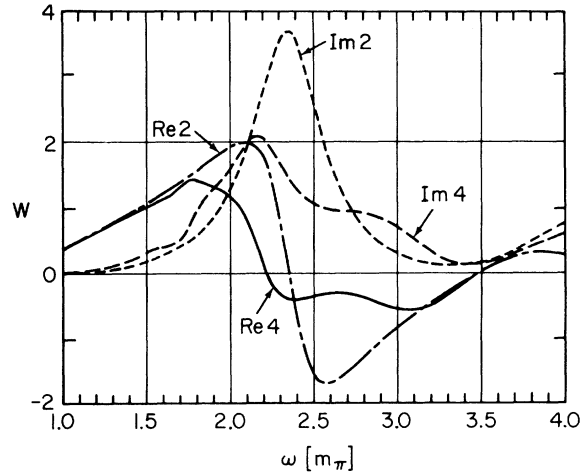


FIG. 19. W resulting from the summation of the local field series (curve 4) compared to the Pauli-corrected W (curve 2).

that the scheme converges quite rapidly. Indeed, we found that the solution has essentially converged after the second iteration.

Finally, Fig. 23 compares the self-consistent W (curve 7) to W calculated with the free $\pi N t$ matrix (curve 1). The resonant mass is slightly larger than the free value, and the resonant width is almost twice the free width. While the imaginary part of the free W is zero at threshold, the imaginary part of the self-consistent W is finite at and below threshold, reflecting the existence of pion absorption channels in the self-consistent equations. This allows us to make some contact between the nuclear matter case and reality.

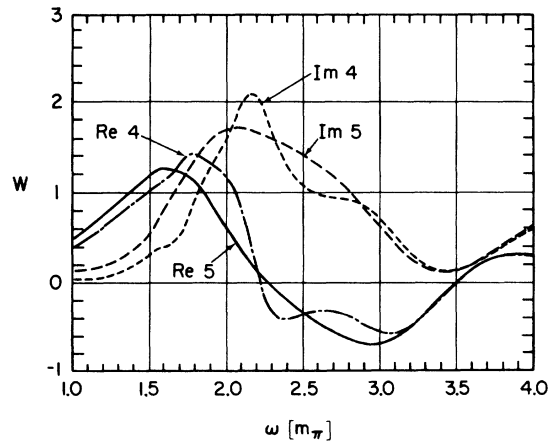


FIG. 20. W resulting from the local field series with pion lines dressed by the Pauli-corrected self energy (curve 5) compared to the local field series without dressing (curve 6). Note the increase in $\text{Im}W$ near threshold ($\omega = m_\pi$) when the pion propagators are dressed.

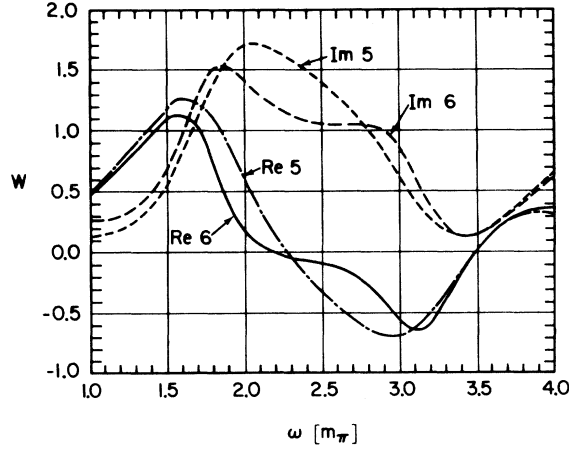


FIG. 21. Comparison of the dressed local field series (curve 5) to a similar calculation where the nucleon recoil mass has been doubled (curve 6). This illustrates the sensitivity of local field effects to nucleon recoil.

From the work of Batty *et al.*,²⁰ on finding a phenomenological optical potential for the pionic atom, it is possible to calculate an empirical value for the imaginary part of W at threshold by using the equation

$$\text{Im}W(m_\pi) = \frac{8\pi M}{2M + m_\pi} (\rho_n + \rho_p)^2 \text{Im}C_0, \quad (27)$$

where $\text{Im}C_0 = 0.0425m_\pi^{-6}$ is the value given by Batty *et al.*, resulting from a fit to the data with a form for the optical potential not including the LLEE correction. Equation (27) gives $\text{Im}W(m_\pi)^{\text{empirical}} = 0.107$, while the self-consistent

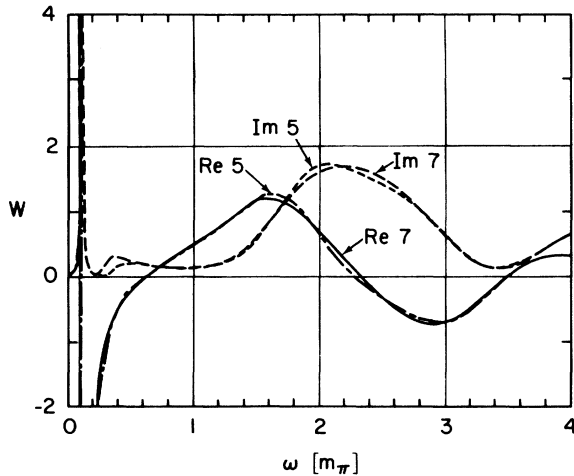


FIG. 22. Comparison of the first iteration of the self-consistent equations (curve 5, same as the dressed local field series) to the converged self-consistent W (curve 7). Complete self-consistent dressing of pion lines results in little difference from dressing of pion lines with the Pauli-corrected self-energy

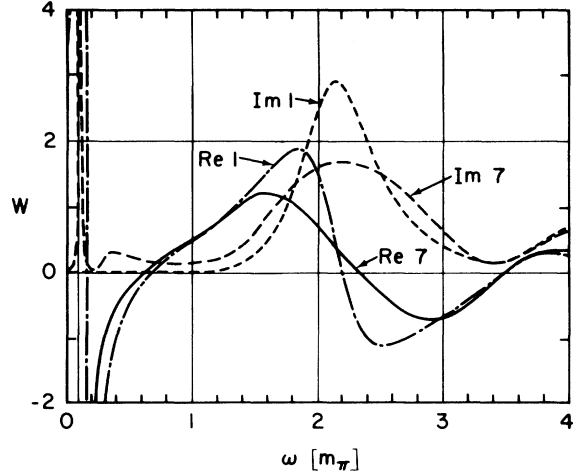


FIG. 23. Comparison of the self-consistent W (curve 7) with the free W (curve 1). Note the broadening of the resonance in the self-consistent quantity and the finite $\text{Im}W$ below threshold which results from absorption.

nuclear matter problem gives $\text{Im}W(m_\pi) = 0.137$. The nuclear matter solution is then within 30% of the empirical value.

Finally, the values of the function W shown in curve 7 of Fig. 23 should not be used directly to construct an optical potential for calculating π -nucleus elastic scattering. Since only the right-hand (uncrossed) contributions to W are displayed, the values of $\text{Re}W$ in the threshold region and below are not adequately described. A minimal treatment of the crossing would be to simply use

$$W^{\text{total}}(k, \omega) = W(k, \omega) + W(k, -\omega). \quad (28)$$

A more complete treatment of the crossing will be left to a future paper.

IV. SUMMARY AND CONCLUSIONS

In summary, we have presented a general approach to the calculation of the self-consistent $\pi N t$ matrix using field theory and Goldstone diagrams. As an illustration of this general theory, a simple solvable case has been presented which treats pion scattering and absorption processes on an equal footing. This model problem does not include contributions from crossed diagrams, correlations, or ρ exchange. A Fermi gas model is used to describe the nucleus, and the $\pi N t$ matrix is chosen to be of a static, factorable, separable form. From this calculation we draw the following conclusions.

(1) Any conclusion of local field effects must allow nucleon recoil. The pion absorption contributions cannot otherwise be included.

(2) All graphs in the local field series must be summed in order to maintain unitarity.

(3) A detailed description of the pion self-energy requires that all internal pion lines must be dressed by at least the first-order optical potential.

(4) Dressing of the internal pion lines increases the imaginary part of the optical potential at threshold by a factor of 3. The dressed value is within 30% of the empirically determined imaginary part of the optical potential.

(5) Dressing of the internal pion lines with the fully self-consistent pion self-energy results in only detailed changes from dressing of the pion lines with only the Pauli-corrected self-energy.

The modification of the $\pi N t$ matrix by the nuclear medium must be taken into account in multiple scattering approaches to the pion optical potential.

Both π -absorption and resonant scattering processes play a substantial role in the local field correction, and the net result is considerable suppression of the imaginary part of the π -nucleus optical potential at the πN resonance energy. Because pion absorption and resonant scattering mechanisms have been treated on an equal footing, the theory is expected to have very interesting implications for the breakdown of reaction cross sections into components due to absorption and inelastic pion scattering. A local density approximation to the self-consistent optical potential will be explored in future work aimed at the explanation of reaction cross sections.

Several extensions of the theory are expected to prove numerically significant but are not expected to alter the qualitative conclusions. One of these is a more complete treatment of Fermi broadening effects which have been emphasized by Shakin and collaborators.¹⁸ However, little additional broadening of the resonance from that calculated in this paper is expected when Fermi effects are included in the calculation of local field effects since the input amplitudes will have effectively a much weaker resonancelike energy dependence. A second refinement of interest is to include the crossed insertions into the theory. Finally, we mention the connection of the present results to earlier work by Banerjee and Wallace on the leading order local field correction in π -¹⁶O scattering. The reflective mechanism that was found to be important in the earlier study is suppressed in the nuclear matter calculation of this paper because the pion may only scatter forward in nuclear matter. Thus, there is a need to re-investigate the reflective parts of the local field correction incorporating the self-consistent $T_{\pi N}$ and dressed pion propagators which will reduce

this effect.

The support of the U. S. Department of Energy and the University of Maryland Computer Science Center is gratefully acknowledged. We wish to acknowledge useful discussions with F. Lenz of some of the aspects of this paper.

APPENDIX A: GOLDSTONE RULES FOR THE π -NUCLEUS t MATRIX

Rules for drawing Goldstone diagrams

1. A Goldstone diagram consists of directed lines for pions, nucleons, and other particles and vertices where three or more of these lines join. If a potential theory for the NN interaction is used, there will be nondirected horizontal lines of specified character connecting two nucleon lines to indicate potential interactions. The types of lines used in this paper are (i) dashed lines for pions; (ii) upward solid lines for nucleons in unoccupied (particle) states, downward solid lines for occupied (hole) states; (iii) horizontal wiggly lines represent G matrices. Single potential lines are never exhibited separately.

2. All of our diagrams will have two external lines, incoming and outgoing pion lines.

In Goldstone diagrams the time sequences of events are maintained. However, in our diagrams for the t matrices, the starting point and end point of the external pion lines are of no significance. The relative time sequences of the first and the last interactions of the external pion lines with the nuclear medium are of significance. The arrows on the external pion lines are drawn only to help the reader distinguish between the incoming and the outgoing lines.

Rules for evaluating the Goldstone diagrams

1. Associate with each internal line an appropriate set of quantum numbers (e.g., spin, isospin, momentum, etc.). The energy of the line is determined by the chosen model Hamiltonian and the quantum numbers. The energy associated with the external pion line is the incoming energy ω .

2. Between successive vertices, there is an energy denominator. To determine these denominators we draw for each diagram an auxiliary diagram where we remove the original external pion lines and then replace them with a single line directed from the exit point (last interaction point of the external line) to the entry point (first interaction point). This line is directed upward or downward depending on the relative time ordering of the first and last interactions. A denominator is equal to the sum of energies of all downward-going lines minus the sum of all upward-

going lines present in the interval.

3. The rules for the vertices and G -matrix interactions are the usual ones.

4. Form the product of all denominators and matrix elements of interactions and sum over all internal variables.

5. The sign of any contribution of any diagram is given by $(-1)^{h+l}$, where h is the number of hole lines and l is the number of closed fermion loops.

APPENDIX B

To illustrate the connection between the nucleon pole shift and the effect of Pauli corrections on mass renormalization, Eq. (18) can be rewritten as

$$H_{2f}^P(k, \omega) = \frac{1}{H_{2f}^{0-1}(\omega) + \mathcal{F}(k, \omega)}. \quad (\text{B1})$$

In the region where H^0 comes primarily from the pole contribution, i.e., near $\omega=0$, the function \mathcal{F} serves to shift the energy of the pole. The relation of this shift to mass renormalization can be seen by considering the segment of some arbitrary Goldstone diagram represented by Fig. 24. In free space the insertion of such a diagram into the nucleon propagator is part of the nucleon mass renormalization, and the nucleon mass counter term in the Lagrangian is chosen to exactly cancel the mass shift due to such an insertion. This implies that the nucleon mass counter term is equal to the insertion represented by Fig. 24. Therefore, this insertion minus the counter term when calculated in the nuclear medium is proportional to

$$\frac{1}{i} \int d^4q \langle p | j_{\mathbf{r}}(0) | p-q \rangle [S_F^{\text{NM}^{(*)}}(p-q) - S_F^{\text{free}^{(*)}}(p-q)] \times S^{(*)}(q) \langle p-q | j_{\mathbf{r}}(0) | p \rangle, \quad (\text{B2})$$

$$\frac{1}{(2\pi)^3} \int \frac{d^4q}{2\omega_q} \frac{\langle p | j_{\mathbf{r}}(0) | p-q \rangle \langle p-q | j_{\mathbf{r}}(0) | p \rangle}{q^0 - \omega_q + i\eta} \delta[p^0 - q^0 - E(\vec{p} - \vec{q})] \theta(k_F - |\vec{p} - \vec{q}|) \\ = \frac{1}{(2\pi)^3} \int \frac{d^3q}{2\omega_q} \frac{\langle p | j_{\mathbf{r}}(0) | p-q \rangle \langle p-q | j_{\mathbf{r}}(0) | p \rangle}{p^0 - E(\vec{p} - \vec{q}) - \omega_q + i\eta} \theta(k_F - |\vec{p} - \vec{q}|) \quad (\text{B7})$$

which is of the same form as the function \mathcal{F} , Eq. (20). If retardation is neglected, (B7) becomes

$$\frac{1}{2(2\pi)^3} \int \frac{d^3q}{\omega_q^3} \langle p | j_{\mathbf{r}}(0) | p-q \rangle \langle p-q | j_{\mathbf{r}}(0) | p \rangle \theta(k_F - |\vec{p} - \vec{q}|), \quad (\text{B8})$$

which can be recognized as the exchange part of the Hartree-Fock potential arising from one pion exchange. The factor of $\frac{1}{2}$ occurs because we have used only the positive frequency part of the pion propagator. Since we have made no attempt to include a potential for excited nucleons, we

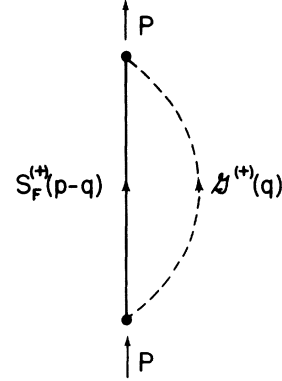


FIG. 24. Nucleon line insertion which is related to nucleon mass renormalization.

where the positive frequency nucleon propagator in nuclear matter is

$$S_F^{\text{NM}^{(*)}}(l) = \frac{\theta(|\vec{l}| - k_F)}{l^0 - E(\vec{l}) + i\eta} + \frac{\theta(k_F - |\vec{l}|)}{l^0 - E(\vec{l}) - i\eta}, \quad (\text{B3})$$

the free positive frequency nucleon propagator is

$$S_F^{\text{free}^{(*)}}(l) = \frac{1}{l^0 - E(\vec{l}) + i\eta} \\ = \frac{\theta(|\vec{l}| - k_F)}{l^0 - E(\vec{l}) + i\eta} + \frac{\theta(k_F - |\vec{l}|)}{l^0 - E(\vec{l}) + i\eta}, \quad (\text{B4})$$

and the positive frequency pion propagator is

$$S^{(*)}(q) = \frac{1}{2\omega_q(q^0 - \omega_q + i\eta)}. \quad (\text{B5})$$

From (B3) and (B4) it is clear that

$$S_F^{\text{NM}^{(*)}}(l) - S_F^{\text{free}^{(*)}}(l) = 2\pi i \delta[l_0 - E(\vec{l})] \theta(k_F - |\vec{l}|). \quad (\text{B6})$$

Using this, (B2) becomes

have made no attempt to subtract this small potential contribution. If a potential for excited nucleons were used, this type of insertion (and many more besides) would have to be canceled by an additional potential counter term.

- ¹K. M. Watson, *Phys. Rev.* **89**, 575 (1953); M. L. Goldberger and K. M. Watson, *Collision Theory* (Wiley, New York, 1964), p. 749; A. K. Kerman, H. McManus, and R. M. Thaler, *Ann. Phys. (N.Y.)* **8**, 551 (1959); R. H. Landau, S. C. Phatak, and F. Tabakin, *ibid.* **78**, 299 (1973); L. C. Liu and C. M. Shakin, *Phys. Rev. C* **16**, 333 (1977); **16**, 1963 (1977); R. H. Landau and A. W. Thomas, *Nucl. Phys.* **A302**, 461 (1978); N. J. DiGiacomo, A. S. Rosenthal, E. Rost, and D. Sparrow, *Phys. Lett.* **66B**, 421 (1977); T.-S. H. Lee, *ibid.* **67B**, 282 (1977).
- ²L. Kisslinger and W. Wang, *Ann. Phys. (N.Y.)* **99**, 374 (1976); M. Hirata, J. H. Koch, F. Lenz, and E. J. Moniz, *Phys. Lett.* **70B**, 281 (1977); *Ann. Phys. (N.Y.)* **120**, 205 (1979); G. E. Brown and W. Weise, *Phys. Rep.* **22C**, 280 (1975).
- ³A. W. Thomas and R. H. Landau, *Phys. Rep.* **58**, 112 (1980).
- ⁴I. Navon *et al.*, *Phys. Rev. Lett.* **42**, 1465 (1979); D. Ashery, in *Proceedings of the Eighth International Conference on High Energy Physics and Nuclear Structure*, edited by D. F. Measday and A. W. Thomas (North-Holland, Amsterdam, 1980); *Nucl. Phys.* **A335**, 385 (1980).
- ⁵L. L. Foldy and J. D. Walecka, *Ann. Phys. (N.Y.)* **54**, 447 (1969).
- ⁶B. D. Keister, *Nucl. Phys.* **A271**, 342 (1976).
- ⁷M. B. Johnson and H. A. Bethe, *Nucl. Phys.* **A305**, 418 (1978).
- ⁸M. B. Johnson and B. D. Keister, *Nucl. Phys.* **A305**, 461 (1978).
- ⁹M. K. Banerjee and S. J. Wallace, *Phys. Rev. C* **21**, 1996 (1980).
- ¹⁰L. S. Celenza, L. C. Liu, W. Nutt, and C. M. Shakin, *Phys. Rev. C* **14**, 1090 (1976).
- ¹¹D. M. Schneider, M. K. Banerjee, J. W. Van Orden, and S. J. Wallace, University of Maryland Report No. PP 81-027 (ORO 5126-118), 1980 (unpublished).
- ¹²J. B. Cammarata and M. K. Banerjee, *Phys. Rev. Lett.* **31**, 610 (1973); *Phys. Rev. C* **13**, 299 (1976). Note that the diagrams in these references are incorrectly drawn. All arrows on pion lines must point in the same direction.
- ¹³B. H. Brandow, *Rev. Mod. Phys.* **39**, 771 (1967).
- ¹⁴D. M. Schneider, M. K. Banerjee, J. W. Van Orden, and S. J. Wallace, University of Maryland Report No. PP 81-024 (ORO 5126-117), 1980 (unpublished).
- ¹⁵E. Oset and W. Weise, *Nucl. Phys.* **A319**, 477 (1979).
- ¹⁶J. M. Eisenberg and D. S. Koltun, *Theory of Meson Interactions with Nuclei* (Wiley, New York, 1980), p. 168.
- ¹⁷H. A. Bethe, B. H. Brandow, and A. G. Petschek, *Phys. Rev.* **129**, 225 (1963).
- ¹⁸R. S. Bhalerao, L. C. Liu, and C. M. Shakin, *Phys. Rev. C* **21**, 2103 (1980).
- ¹⁹H. A. Bethe, *Phys. Rev. Lett.* **30**, 105 (1973).
- ²⁰C. J. Batty, S. F. Biaci, E. Friedman, S. D. Hoath, J. D. Davies, G. J. Pyle, G. T. A. Squier, D. M. Asbury, and A. Guberman, *Nucl. Phys.* **A332**, 445 (1979).